

## Investigations and Improvements of AlInN/GaN HEMTs Grown on Si

Jen-Inn Chyi<sup>a</sup>, Yue-Ming Hsin<sup>a</sup>, Geng-Yen Lee<sup>a</sup>, and Hsien-Chin Chiu<sup>b</sup>

<sup>a</sup>Department of Electrical Engineering, National Central University, Taiwan, R.O.C.

<sup>b</sup>Department of Electronic Engineering, Chang Gung University, Taiwan, R.O.C.

Email:chy@ee.ncu.edu.tw

This paper reports our continuous efforts and achievements in understanding and improving AlInN/AlN/GaN heterostructure for high performance field-effect transistors and switching devices. AlInN/AlN/GaN high electron mobility transistors (HEMTs) with high electron mobility and low sheet resistance have been demonstrated on 6" Si(111) substrates. It is found that electron mobility of AlInN/AlN/GaN HEMTs is closely related to the presence and quality of the AlN spacer layer, which determines the dominant carrier scattering mechanism. A comparative study on the electrical characteristics of AlInN/AlN/GaN and AlGaIn/GaN metal-insulator-semiconductor (MIS)-HEMTs shows that both devices exhibit similar low-frequency noise behavior and no obvious generation-recombination (g-r) noise component, implying carrier number fluctuation is the dominant noise mechanism in both structures.

### Introduction

GaN-based high electron mobility transistors (HEMTs) have attracted tremendous attention because of its wide bandgap and high power handling capability, which are the two fundamental merits for power electronics applications. Lattice-matched AlInN/GaN heterostructure has been considered a promising alternative to its AlGaIn/GaN counterpart due to its stronger spontaneous polarization, which induces higher carrier concentration and therefore reduces channel resistance [1]. In addition, AlInN lattice-matched to GaN would not suffer from the inverse piezoelectric effect that deteriorates device reliability as observed on AlGaIn/GaN HEMTs [2]. While a few excellent device characteristics have been demonstrated over the years [3, 4], AlInN/GaN HEMTs are still in general more vulnerable than AlGaIn/GaN HEMTs. It is desirable to clarify the origin(s) of this problem to expedite the development of high power AlInN/GaN HEMTs and the devices alike. In this work, we report our recent study on the growth and electrical characterization of AlInN/GaN HEMTs so that better understanding of this heterostructure can be achieved for further improvements in device performance.

### Epitaxial Growth and Electron Mobility

Growing high quality AlInN/AlN/GaN HEMTs is in general more difficult than growing its AlGaIn/GaN counterparts due to the strong immiscibility effect between AlN

and InN, especially when growing on Si substrates. The immiscibility effect tends to induce alloy fluctuation and rough interface near the two-dimensional electron gas channel and deteriorate electron mobility. Improving surface roughness is therefore regarded as a key task to enhance electron mobility. To dates, a number of efforts have been made to improve the surface roughness of AlInN by adjusting its growth parameters [5, 6]. Our observations indicate that the roughness may result from a rough GaN layer beneath the AlInN layer.

To clarify the influence of each layer on electron mobility, three AlInN/AlN/GaN HEMTs, denoted as sample A, B, and C, are prepared by metal-organic chemical vapor deposition on 6 inch Si (111) substrates. Sample A is a reference structure, consisting of a 1.25  $\mu\text{m}$  AlN/AlGaIn composite buffer layer followed by a 2.5  $\mu\text{m}$  GaN undoped buffer layer, and a 10 nm AlInN Schottky layer with 81.9 % of AlN, that makes the layer lattice matched to GaN. While using the same structure and growth conditions (conditions I) for sample B, a 1.5-nm AlN spacer layer is grown on the GaN buffer right before the growth of the AlInN Schottky layer. The Hall-effect measurement results shown in Table I indicate that the electron mobility of sample B is greatly enhanced from sample A's 484 to 1220  $\text{cm}^2/\text{V}\cdot\text{s}$ , illustrating the critical role of this AlN spacer layer. Since atomic force microscopy (AFM) measurements, as depicted in Fig. 1, show that the root-mean-square (RMS) roughness of sample B is 1.66 nm, which is much larger than the 0.46 nm of sample A, the enhancement in the electron mobility of sample B is attributed to the reduced alloy scattering by the AlN spacer, which separates the two-dimensional electron gas (2DEG) from the AlInN Schottky layer. The low mobility observed on sample A is likely dominated by strong alloy scattering. This scattering process is thought more pronounced in the AlInN HEMTs grown on Si substrates than sapphire substrates as more dislocations, which cause indium fluctuation, are observed on the ones grown on Si substrates [7].

To investigate the effect of roughness scattering on mobility, a sample of half structure, i.e. without the AlInN barrier layer, is grown to assess the roughness of the AlN spacer layer. AFM measurement shows that the surface of the AlN layer has an RMS roughness of 0.89 nm and many pits. This implies electron mobility could be further improved if the roughness and defect are reduced. A new set of growth conditions (condition II) is then developed for sample C aiming at maintaining a smooth AlN spacer layer. This results in a full HEMT structure with an improved RMS roughness of 0.738 nm and an increased mobility to 1360  $\text{cm}^2/\text{V}\cdot\text{s}$  without sacrificing its 2DEG density ( $2.13 \times 10^{13} \text{ cm}^{-2}$ ), leading to a very low sheet resistance of 215  $\text{ohm}/\text{sq}$ . Given the excellent electrical properties of the AlInN HEMTs obtained in this work, further improvement in electron mobility is expectable if the growth conditions are optimized for each layer in the structure.

Table 1. AFM and Hall measurement results of the three types of AlInN HEMT structures

Structure	RMS (nm)	Mobility 300K ( $\text{cm}^2/\text{V}\cdot\text{s}$ )	Carrier concentration 300K ( $\text{cm}^{-2}$ )	Sheet resistance 300K ( $\Omega/\square$ )
AlInN/GaN	0.458	484	$2.06 \times 10^{13}$	625
AlInN/AlN/GaN (conditions I)	1.664	1220	$1.85 \times 10^{13}$	276
AlInN/AlN/GaN (conditions II)	0.738	1360	$2.13 \times 10^{13}$	215

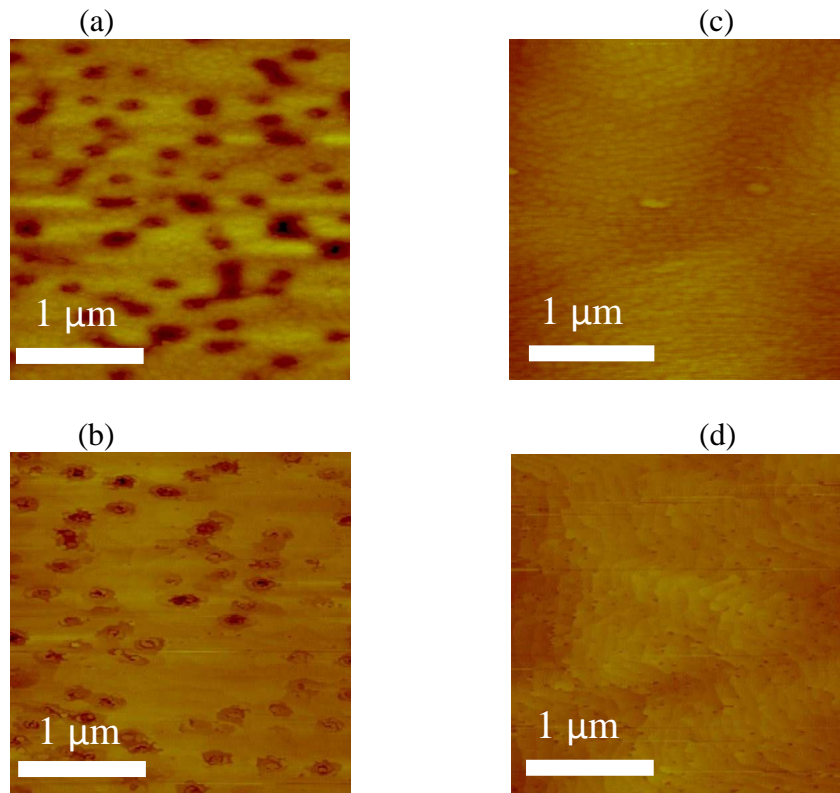


Fig 1. AFM images of the surface morphology of (a) AlInN/AlN/GaN (conditions I) (b) AlN/GaN (conditions I) (c) AlInN/AlN/GaN (conditions II) (d) AlN/GaN (conditions II)

### Electrical Characteristics of AlInN and AlGaN MIS-HEMTs

In order to further investigate and distinguish the trap characteristics of InAlN and AlGaN-based HEMTs, MIS-HEMTs with InAlN and AlGaN barrier layers are subject to low frequency noise measurements. Fig. 2 (a)-(b) shows the cross-section of the MIS-HEMTs. The  $\text{Al}_2\text{O}_3$  gate dielectric is deposited by atomic layer deposition (ALD). Both types of devices have a gate length of  $2 \mu\text{m}$  with gate to source and gate to drain distance of  $3.5 \mu\text{m}$  and  $20 \mu\text{m}$ , respectively.

Fig. 3 (a)-(d) shows the typical DC characteristics of both devices. The maximum drain current is over  $500 \text{ mA/mm}$  at  $V_{\text{DS}}=10 \text{ V}$  and  $V_{\text{GS}}=2 \text{ V}$  for both devices. The threshold voltage of the AlGaN and AlInN device is  $-7.1 \text{ V}$  and  $-5.3 \text{ V}$ , respectively. The gate leakage current ( $I_{\text{GS}}$ ) of the AlInN device is three orders of magnitude higher than that of the AlGaN device at  $V_{\text{GS}}= -8 \text{ V}$ . The off-state breakdown voltage ( $V_{\text{BR}}$ ) is defined at which the  $I_{\text{DS}}$  reaches  $1 \text{ mA/mm}$  as  $V_{\text{GS}}= -10 \text{ V}$ . The  $V_{\text{BR}}$  of AlInN and AlGaN device is  $425$  and  $568 \text{ V}$ , respectively.

Figure 4(a) shows the frequency-dependent normalized drain current noise ( $S_{\text{ID}}/I_{\text{DS}}^2$ ) at various  $V_{\text{GS}}-V_{\text{TH}}$  with  $V_{\text{DS}}= 1 \text{ V}$  (linear region) for the AlGaN and AlInN MIS-HEMTs. The figure reveals no obvious generation-recombination (g-r) noise component in both devices. The AlInN device has a lower noise spectral density than that of the AlGaN though. Figure 4(b) shows the normalized drain current noise density versus gate

overdrive voltage at 100 Hz. The slope of  $S_{ID}/I_{DS}^2$  in this figure is  $-1.65$  and  $-1.66$  for the AlInN and AlGaN MIS-HEMT, respectively, implying that carrier number fluctuation is the dominant noise mechanism in both structures. Further investigations on the trap distribution in the devices are undertaken and the results will be reported later.

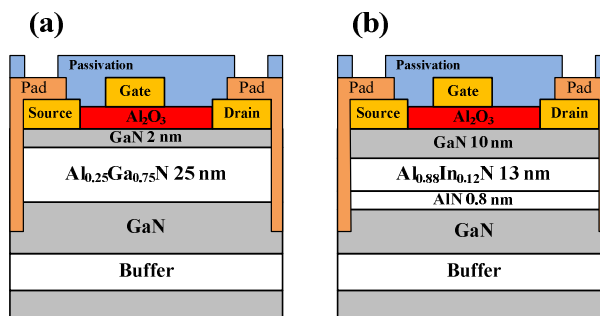


Fig. 2 Cross-sectional views of the (a) AlGaN/GaN and (b) AlInN/AlN/GaN MIS-HEMTs

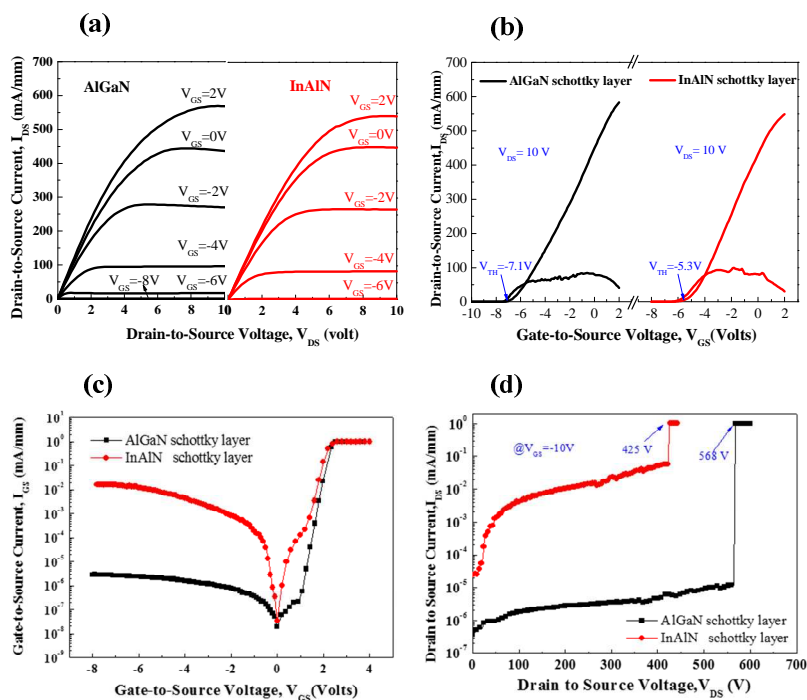


Fig. 3 Typical (a)  $I_{DS}$ - $V_{DS}$ , (b)  $I_{DS}$ - $V_{GS}$ , (c)  $I_{GS}$ - $V_{GS}$  and (d) off-state breakdown characteristics of the AlGaN and AlInN MIS-HEMTs

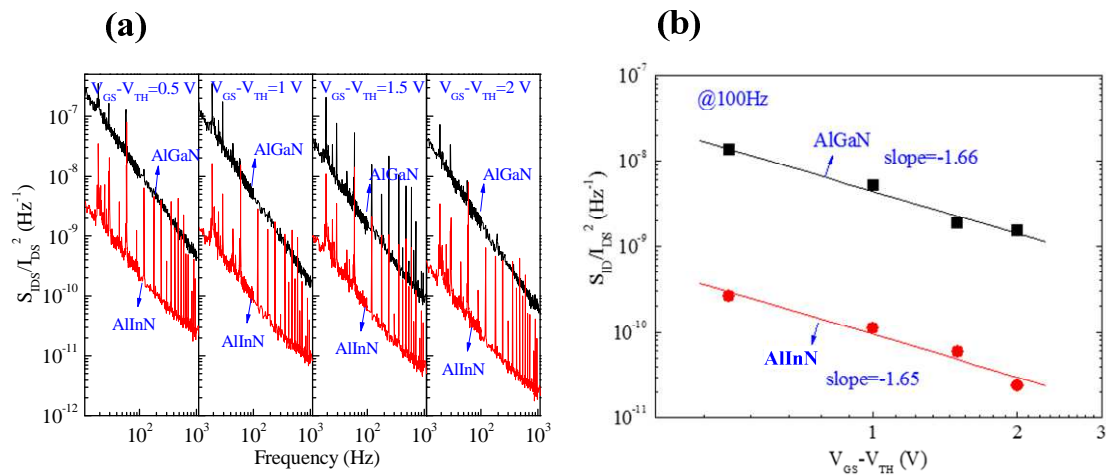


Fig. 4 (a) Normalized drain current noise ( $S_{ID}/I_{DS}^2$ ) versus  $V_{GS} - V_{TH}$  at  $V_{DS} = 1$  V (linear region) for traditional AlGaIn/GaN HEMT and AlInN/GaN HEMT, (b) Normalized drain current noise ( $S_{ID}/I_{DS}^2$ ) versus gate overdrive voltage at 100 Hz

## Conclusions

AlInN/AlN/GaN heterostructure with high electron mobility and low sheet resistance have been demonstrated on 6" Si(111) substrates. Our findings show that electron mobility of AlInN/AlN/GaN HEMTs is closely related to the presence and quality of the AlN spacer layer, which is involved with the interplay of alloy scattering and roughness scattering. By perfecting the crystal quality and smoothness of the AlN spacer layer, AlInN HEMTs having electron mobility of 1360 cm<sup>2</sup>/V-s with two-dimensional electron gas density of  $2.13 \times 10^{13}$  cm<sup>-2</sup> and sheet resistance of 215 ohm/sq have been achieved.

Besides, a comparative study on the electrical characteristics of AlInN/AlN/GaN and AlGaIn/GaN metal-insulator-semiconductor (MIS)-HEMTs shows that both devices exhibit similar low-frequency noise behavior and no obvious generation-recombination (g-r) noise component, implying carrier number fluctuation is the dominant noise mechanism in both structures.

## Acknowledgments

The authors would like to thank the National Science Council of Taiwan R.O.C. for the financial support under Contract No. NSC 102-2622-E-008-012-CC1 and NCU-DEL-102-A-07.

## References

- [1] J. Kuzmik, "Power electronics on InAlN/(In)GaIn: Prospect for a record performance," *IEEE Electron Device Letters*, vol. 22, no. 11, pp. 510-512, 2001.
- [2] J. Jungwoo, and J. A. del Alamo, "Critical Voltage for Electrical Degradation of GaN High-Electron Mobility Transistors," *IEEE Electron Device Letters*, vol. 29, no. 4, pp. 287-289, 2008.

- [3] F. Medjdoub, J. F. Carlin, M. Gonschorek, E. Feltin, M. A. Py, D. Ducatteau, C. Gaquiere, N. Grandjean, and E. Kohn, "Can InAlN/GaN be an alternative to high power / high temperature AlGaIn/GaN devices?," pp. 1-4, 2006.
- [4] D. S. Lee, X. Gao, S. Guo, D. Kopp, P. Fay, and T. Palacios, "300-GHz InAlN/GaN HEMTs With InGaIn Back Barrier," *IEEE Electron Device Letters*, vol. 32, no. 11, pp. 1525-1527, 2011.
- [5] M. Gonschorek, J. F. Carlin, E. Feltin, M. A. Py, and N. Grandjean, "High electron mobility lattice-matched AlInN/GaN field-effect transistor heterostructures," *Applied Physics Letters*, vol. 89, no. 6, pp. 062106, 2006.
- [6] M. Hiroki, N. Maeda, and T. Kobayashi, "Fabrication of an InAlN/AlGaIn/AlN/GaN Heterostructure with a Flat Surface and High Electron Mobility," *Applied Physics Express*, vol. 1, pp. 111102, 2008.
- [7] T. Kehagias, G. P. Dimitrakopoulos, J. Kioseoglou, H. Kirmse, C. Giesen, M. Heuken, A. Georgakilas, W. Neumann, T. Karakostas, and P. Komninou, "Indium migration paths in V-defects of InAlN grown by metal-organic vapor phase epitaxy," *Applied Physics Letters*, vol. 95, no. 7, pp. 071905, 2009.